Mycorrhiza (2020) 30:229–242
https://doi.org/10.1007/s00572-020-00956-w

ORIGINAL ARTICLE

HyLength: a semi-automated digital image analysis tool for measuring the length of roots and fungal hyphae of dense mycelia

Alessio Cardini[1] · Elisa Pellegrino[1] · Emanuela Del Dottore[2] · Hannes A. Gamper[1,3] · Barbara Mazzolai[2] · Laura Ercoli[1]

Received: 10 January 2020 / Accepted: 30 March 2020 / Published online: 16 April 2020

Abstract

In plant-fungus phenotyping, determining fungal hyphal and plant root lengths by digital image analysis can reduce labour and increase data reproducibility. However, the degree of software sophistication is often prohibitive and manual measuring is still used, despite being very time-consuming. We developed the *HyLength* tool for measuring the lengths of hyphae and roots in in vivo and in vitro systems. The *HyLength* was successfully validated against manual measures of roots and fungal hyphae obtained from all systems. Compared with manual methods, the *HyLength* underestimated *Medicago sativa* roots in the in vivo system and *Rhizophagus irregularis* hyphae in the in vitro system by about 12 cm per m and allowed to save about 1 h for a single experimental unit. As regards hyphae of *R. irregularis* in the in vivo system, the *HyLength* overestimated the length by about 21 cm per m compared with manual measures, but time saving was up to 20.5 h per single experimental unit. Finally, with hyphae of *Aspergillus oryzae*, the underestimation was about 8 cm per m with a time saving of about 10 min for a single germinating spore. By benchmarking the *HyLength* against the *AnaMorf* plugin of the *ImageJ/Fiji*, we found that the *HyLength* performed better for dense fungal hyphae, also strongly reducing the measuring time. The *HyLength* can allow measuring the length over a whole experimental unit, eliminating the error due to sub-area selection by the user and allowing processing a high number of samples. Therefore, we propose the *HyLength* as a useful freeware tool for measuring fungal hyphae of dense mycelia.

Keywords Digital image analysis · Plant-fungus phenotyping · Root length · Hyphal length · Arbuscular mycorrhizal fungi · Extraradical mycelium

Introduction

Root and fungal hyphal uptake of mineral nutrients and water varies in time and space, depending on the environmental conditions (Augé 2004; Smith et al. 1994; van Vuuren et al. 1997; Ercoli et al. 2017; Coccina et al. 2019). Determining root and fungal hyphal lengths is a basic undertaking in many ecophysiological and ecological studies (Jakobsen et al. 1992; Tibbett 2000; Allen and Kitajima 2013). Traditionally, total length of filamentous objects is estimated manually by the grid-line intersect method using the Newman formula: Length $= \frac{\pi N A}{2 H}$, where N is the number of intersections of filamentous objects with reference lines of length H in the measurement area A (Newman 1966). A precondition that this formula can be applied is that the filamentous objects are randomly spread across the measurement area, which is not the case for in situ images of root systems and fungal mycelia. Approaching this methodology manually is time-consuming, and it usually constrains the size and number of samples that can be processed, compromising the accuracy and precision of root and fungal hyphal length measurements and consequently

Electronic supplementary material The online version of this article (https://doi.org/10.1007/s00572-020-00956-w) contains supplementary material, which is available to authorized users.

✉ Elisa Pellegrino
elisa.pellegrino@santannapisa.it

[1] Institute of Life Sciences, Scuola Superiore Sant'Anna, Piazza Martiri della Libertà 33, 56127 Pisa, Italy

[2] Center for Micro-BioRobotics, Istituto Italiano di Tecnologia, Viale Rinaldo Piaggio 34, 56025 Pontedera, Pisa, Italy

[3] Present address: Free University of Bozen-Bolzano, Faculty of Science and Technology, Universitätsplatz 5 - piazza Università 5, 39100 Bozen-Bolzano, Italy

the likelihood of discovering biological differences and treatment effects. Hence, automated and semi-automated image analyses could save time, increasing comparability and consistency of data.

Since the advent of digital imaging and computing, considerable effort has been made to establish workflows and design (semi-)automated tools to determine the length of roots and hyphae, as well as of other filamentous structures (e.g. Green et al. 1994; Himmelbauer 2004; Meijering et al. 2004; Barry et al. 2009; Lobet et al. 2013; Pierret et al. 2013; Barry et al. 2015; Betegón-Putze et al. 2019). To avoid the necessity to arrange filamentous objects randomly before image acquisition or to enable analyses of images under in situ conditions, modern tools use skeletonisation of filamentous objects to one-pixel threads and count pixels to determine lengths (e.g. Pierret et al. 2013; Barry et al. 2015). Examples of available tools making use of pixel counting in skeletonised digital images of roots and fungal hyphae are the *WinRhizo* (Arsenault et al. 1995; in which the grid-line intersection-based estimation is also available), *RootLM* (Qi et al. 2007), *SmartRoot* (Lobet et al. 2011), *RootTrace* (Naeem et al. 2011), *IJ_Rhizo* (Pierret et al. 2013), *AnaMorf* (Barry et al. 2015) and *HyphaTracker* (Brunk et al. 2018). All the above tools are developed for multiple purposes and analyses going beyond total root/hyphal length determination, such as structural, architectural and growth measurements. Moreover, a tool developed for cell and tissue structural analyses, such as the *Leaf Image Analysis Interface* (*LIMANI*, Dhondt et al. 2012), also has an option to detect and determine the lengths of filamentous objects, such as hyphae of pathogenic fungi. However, manual tracing still is used when imaging and computing systems are unavailable, or training on the latter is lacking. The use of a simple and free interface aiding in root and hyphal length assessments would help to reduce the tediousness of this operation, reducing the time effort. The *ImageJ/Fiji* tool and its *NeuronJ* plugin are examples of freely available and often used software assisting manual tracing (Meijering et al. 2004; Shen et al. 2016).

Nevertheless, most of the above-mentioned tools, including the *ImageJ/Fiji*, have complex interfaces, are highly sophisticated or are dedicated to specialised tasks (Lobet et al. 2013), and only few of them are thoroughly validated and benchmarked for total object length measurement (Lobet 2017; Rose and Lobet 2019). For measuring total fungal hyphal lengths, the only validated software is the *AnaMorf* v.2.017 (Barry et al. 2009, 2015; Barry and Williams 2011), a plugin of the *ImageJ/Fiji* (Schindelin et al. 2012; Schneider et al. 2012). However, the *AnaMorf* was validated with low-density images of germinating hyphae of the saprobic, filamentous fungus *Aspergillus oryzae*, growing on nitrocellulose membranes. Therefore, there is a need to develop user-friendly, validated and benchmarked image analytical tools to measure the length of complex filamentous structures, such as the hyphal network of arbuscular mycorrhizal fungi (AMF).

After colonising plant roots, the AMF develop an extraradical mycelium (ERM) consisting of a complex and extensive network of hyphae spreading throughout the soil (Smith and Read 2008). The connection between the ERM and intraradical fungal structures results in an active symbiotic transport of carbohydrates and lipids to the fungus and mineral nutrients to the plant (Bago et al. 2000; Koide and Mosse 2004). The active role of the AMF in the uptake and transport of minerals needed for plant growth has been demonstrated for P, N, S, K, Zn, Cu, Fe and Mn in various plant/AMF isolate combinations (e.g. P: George et al. 1995, Smith and Smith 2012; N: Hodge et al. 2010, S: Allen and Shachar-Hill 2009; K: Zhang et al. 2017; Zn: Bürkert and Robson 1994, Coccina et al. 2019; Cu: Li et al. 1991; P, N, K, Zn, Cu, Fe and Mn: Miransari et al. 2009; Fe, Cu and Mn: Lehmann and Rillig 2015; and Cu, Zn, Mn and Fe: Liu et al. 2000).

In this study, we developed a user-friendly tool for measuring the length of roots and fungal mycelia, assembling functions of the *Image Processing Toolbox* of MATLAB R2019b (The MathWorks Inc., Natick, MA, USA) that allow skeletonising objects before counting their total pixel number. This tool, named *HyLength*, was validated with four sets of digital images of roots and fungal mycelia grown in in vivo and in vitro systems. The validation was done by comparing the lengths determined by the *HyLength* against those manually determined using either objects traced by the *ImageJ/Fiji* or grid-line intersection counting, which are the standard approaches in this field and represent the reference methods. The measuring times of the different methods were recorded and compared. As additional analysis, we also benchmarked our tool with the currently available similar tool by comparing the lengths determined by the *HyLength* with those determined by the *AnaMorf*. This allowed assessing whether the *HyLength* could perform better than the *AnaMorf*. The MATLAB source code of the *HyLength* is available for free under the general public licence agreement from https://gitlab.iit.it/EDelDottore/hylength, where also, all analysed images are available for downloading to enable further comparisons and optimisation of the tool.

Materials and methods

Experimental set-up: In vivo two-dimensional model system and in vitro three-dimensional model system

The plant species used was *Medicago sativa* var. Messe. The arbuscular mycorrhizal (AM) fungus was *Rhizophagus irregularis* (Błaszk., Wubet, Renker & Buscot) Schüßler and Walker (2010), isolates SW101 and MUCL 41833.

Spores were extracted from pot-culture soil by wet-sieving and decanting, down to a mesh size of 100 μm, flushed into Petri dishes and manually collected with forceps under a Wild dissecting microscope (Leica, Milano, Italy). They were washed by vortexing in sterile distilled water (SDW) for 20 s, rinsed three times in SDW and germinated in the dark at 24 °C between two 47-mm-diameter cellulose nitrate Millipore™ membranes (pore diameter 0.45 μm) placed on acid-washed, autoclaved quartz grit (2–5 mm diameter) in 14-cm-diameter Petri dishes (Avio et al. 2006). Spore clusters (15 clusters each comprising a mean of four spores per cluster) were placed in 13 membrane sandwiches.

Surface-sterilised seeds of *M. sativa* were germinated in moist sterile grit. After 21 days, the root system of one seedling was inserted within one membrane sandwich ($n = 13$), containing the germinated spore clusters showing homogeneous hyphal lengths (Avio et al. 2006; Giovannetti et al. 2006; Pellegrino et al. 2010). Membrane sandwiches were placed into 10-cm-diameter pots (one per pot) filled with sterile quartz grit. Pots were placed in a climate chamber (23 °C day and 18 °C night temperature, 16 h day and 8 h night photoperiod regimes, 70% relative humidity, 400 μmol m^{-2} s^{-1} photosynthetic photon flux density). After 8 weeks, plants were transferred into new membrane sandwiches between two 140-mm-diameter cellulose nitrate Millipore™ membranes (pore diameter 0.45 μm) and maintained in the growth chamber. No fertilisation was applied. After 8 weeks, the membranes were opened, and the roots and the extraradical mycelium were stained with trypan blue in lactic acid (0.05%) to enhance their contrast with the nitrocellulose membrane background.

In the in vitro three-dimensional model system, the plant species used was *Medicago truncatula* cv. Jemalong (line J5). The line was provided by the Institut National de la Recherche Agronomique (INRA, Dijon, France). The AMF isolate utilised was *Rhizophagus irregularis* MUCL 41833 provided from the Glomeromycota In vitro Collection (GINCO) (BCCM™/MUCL, Microbiology Unit, Université catholique de Louvain, Belgium). Seeds of *M. truncatula* were surface-sterilised, and one pre-germinated seedling (5 days old) was placed on a Petri dish (92 mm diameter) filled with modified Strullu-Romand (MSR) medium, lacking sucrose and vitamins and solidified with 3 g L^{-1} of Gellan Gum (Alfa Aesar, Karlsruhe, Germany) sterilised (121 °C) for 20 min (Declerck et al. 1998; Cranenbrouck et al. 2005; Voets et al. 2005). The shoots of seedlings were allowed to grow outside the Petri dishes through a hole made in the dishes, which was closed with silicon grease. The Petri plates were sealed using a Parafilm. After 2 weeks, the *M. truncatula* seedlings were inoculated with 100 spores of *R. irregularis* MUCL 41833. The plates were covered with aluminium foil and grown for 16 weeks in a climate chamber (22 °C day and 18 °C night temperature, 16 h day and 8 h night photoperiod regimes, 80% relative humidity, 120 μmol m^{-2} s^{-1} photosynthetic photon flux density).

Image acquisition of root systems and mycelia

Thirteen images of *M. sativa* root systems and twenty images of subareas of the low-density extraradical mycelium of *R. irregularis* SW101 (Fig. 1) obtained from the in vivo system were taken. Twenty-five images of subareas of the high-density extraradical mycelium of *R. irregularis* MUCL 41833 obtained from the in vitro system also were taken from 25 Petri dishes (one per Petri dish in subareas where only hyphae were present). To account for the partial three-dimensional development of the in vitro mycelium, 15 Z-stacked images (overall depth of about 5 mm) of approximately 20 mm^2 were taken and merged to a projection image in the Leica Application Suite (LAS) v.3.6.0. In addition, 12 images of low-density germinated hyphae of the saprobic, filamentous fungus *Aspergillus oryzae* ATTC 12891 grown on solid growth medium by Barry et al. (2015) were downloaded from https://bitbucket.org/djpbarry/anamorf/downloads/ and used as reference images. Details about image backgrounds and objects, object diameter, image resolution and size as well as the acquisition hardware utilised are given in Table 1. The *A. oryzae* images have already been used to validate the *AnaMorf ImageJ/Fiji plugin* (Barry et al. 2015). All the image analyses and all the software utilised for this work were run on the same laptop with the following specifications: Intel® Core™ i7-7500U Processor, 8-GB RAM, 250-GB SSD, Windows 10 Home 64 bit.

Development of *HyLength*: A new tool for measuring the length of roots and fungal hyphae of dense mycelia

We developed the *HyLength*, a semi-automated digital image tool for measuring the length of roots and fungal mycelia in different experimental systems, assembling existing functions of the Image Processing Toolbox of MATLAB R2019b (Mathworks Inc. 2019). The tool is provided in the form of MATLAB code and runs in a simple one-window user interface (Fig. 2a), which provides easy access to basic image processing commands and utilities. Both the source code and the installer for the stand-alone application are available for download at https://gitlab.iit.it/EDelDottore/hylength. The git repository also contains several sets of different types of pictures of hyphae, roots and other filamentous structures that have been used for validation and benchmarking, either coloured, grey scale or black and white, having different resolutions and dimensions. A README file is present with instructions for installation and execution.

For an image analysis, the suggested measuring workflow is summarised in the flowchart of Fig. 3 with concise code comprising the following steps:

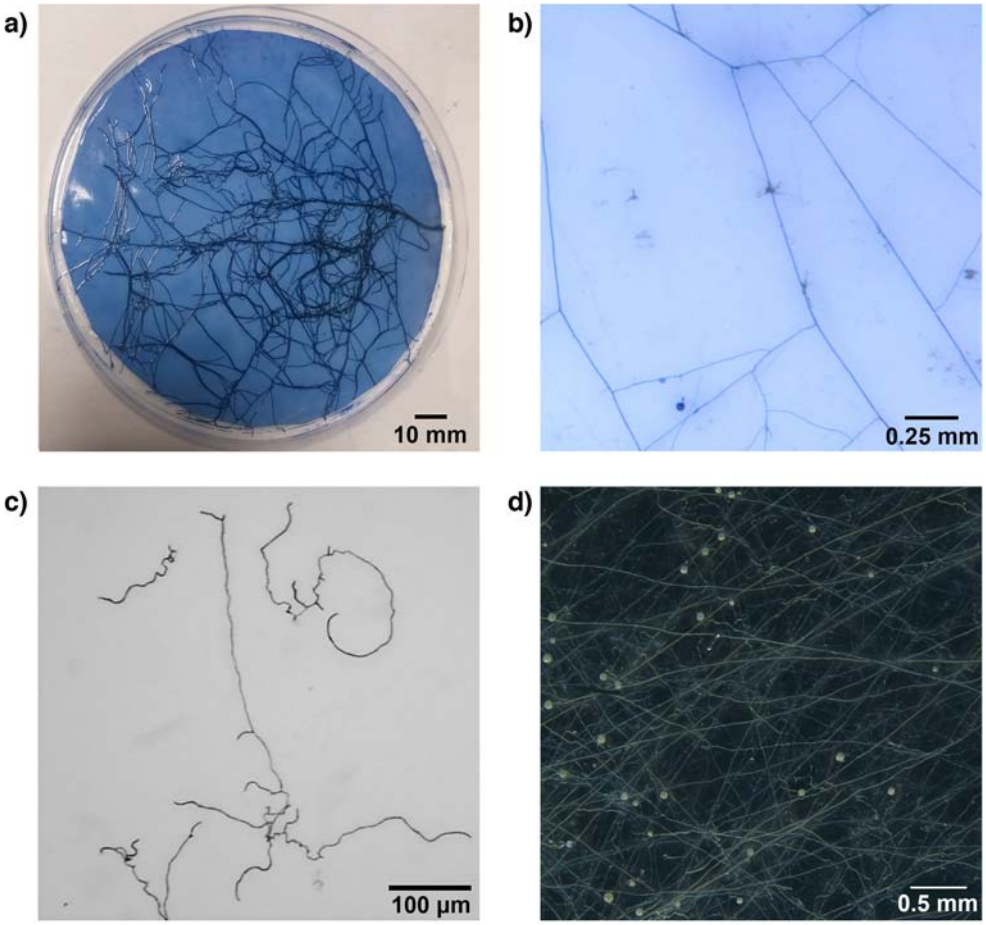

Fig. 1 Examples of the four sets of analysed digital images. **a** Stained root system of *Medicago sativa* L. grown between two nitrocellulose membranes. **b** Subsection of **a** at higher magnification, showing the extraradical mycelium of the arbuscular mycorrhiza fungus *Rhizophagus irregularis* (Blaszk., Wubet, Renker & Buscot) C. Walker & A. Schüßler (strain SW101, × 50). **c** Germination hyphae of the saprobic filamentous fungus *Aspergillus oryzae* (Ahlb.) Cohn (strain ATTC12891) grown on nitrocellulose membrane on malt agar medium (× 100, courtesy: Barry et al. 2009). **d** Mature mycelium of *R. irregularis* (strain MUCL 41833) grown on transparent modified Strullu and Romand solid medium (× 25, z-stack of 15 images). See Table 1 for further details about the image properties

1. Load the image file for the analysis (any image file format is allowed, e.g. jpg, png, tif, tiff, bmp, gif) (Fig. 2b, e). This is allowed by the open file button in the user interface. This operation reads a grey scale, black and white or colour image from the file, with no limit imposed on the size or resolution.
2. Delimit the region of interest using the crop button (Fig. 2a) or the cross cursor which is also automatically

Table 1 Characteristics of the images of filamentous objects utilised for length measurement and for the validation and benchmarking of the semi-automated digital image analysis pipeline *HyLength*

Plant or fungus	Experimental set-up/background	Image subject	Object diameter (pixel)	Image resolution (dpi)	Image size (pixel)	Hardware for image acquisition
Medicago sativa L.	In vivo system /nitrocellulose membrane	Stained root system	2–10	72	2984 × 2408	Samsung SM-A520F mobile phone
Rhizophagus irregularis SW101	In vivo system /nitrocellulose membrane	Stained extraradical mycelium	5–10	300	2560 × 1920	Leica DFC295 camera attached to Leica M205C d issecting microscope (× 20)
Aspergillus oryzae ATTC 12891	In vitro system /nitrocellulose membrane	Stained mycelium	1–2	72	640 × 480	Canon PowerShot S50 camera attached to Leica DM LS2 dissecting microscope (× 100)
Rhizophagus irregularis MUCL 41833	In vitro system/modified Strullu-Romand medium	Extraradical mycelium	2–12	300	2560 × 1920	Leica DFC295 camera attached to Leica M205C dissecting microscope (× 20)

enabled after step 1. With this operation, the user can crop the picture, reducing the dimensions and easing the processing. It also can be a first noise removal step, since only a smaller portion of the picture containing the objects to be analysed is selected. Once the rectangular region has been selected, a double click inside the selected region will confirm the selection and a new window with the working figure (titled "modified") will show. The original picture will still be available (as a comparative reference) in another window titled "Original".

3. Set the scale of the image with the ruler button (Fig. 2a) to define the correspondence between pixels and millimetres. The ruler is defined by the user simply drawing a line on the image in correspondence to a reference element (e.g. an object of known dimension like a ruler or graph paper) and by evaluating the Euclidean distance in pixels between the positions of the extremities of this line. When the ruler is selected, the interface will automatically pop-up the "original" picture. The ruler should be selected above this figure.
4. Convert the image to an 8-bit grey-scale image with the grey button (Fig. 2a). This operation is optional. It depends on the input image if already being coloured and on the quality of the result when applied.
5. Remove non-target objects to avoid spurious length calculations from the selected area with the remove internal area button or outside the selected area with the remove external area button (Fig. 2a). For these operations, the user needs to delimit the area to be removed (or kept) by drawing its boundaries in freehand. Different from the crop operation (step 2), the user can draw an irregular path to exclude undesired irregular artefacts in the picture which might appear between the objects to be analysed or outside the margins of the objects (e.g. hyphae or roots).
6. Covert to black and white with the BW button (Fig. 2a). Pressing the BW button will show new options to set the grey threshold to separate objects (roots and fungal hyphae) from the background on the whole image by Global Threshold, or individually on four quadrants of the image by 4-sub Thresholds, if there are zones with different light exposures. This operation not only converts the image to black and white, but it also helps defining a better contour of the relevant objects in the picture. This operation is crucial for a correct object length count and the user might need to adjust the threshold value with trial and error to improve the result. The operation is then accepted with the apply button or cancelled with the cancel button.
7. Invert black to white pixels and vice versa (Fig. 2c, f) with the invert button (Fig. 2a).
8. Skeletonise all objects to one-pixel (Fig. 2d, g) width with the skeletonise button (Fig. 2a). This operation requires step 7 to have been applied in order to obtain a white object above a black background.
9. Set a minimum pixel (px) threshold to remove noise by clear area with less than (px) button (Fig. 2a). The number of pixels must be specified (we suggest a pixel value ranging from two to five).
10. Count the pixels to obtain the length with the count length button (Fig. 2a) and read the length from the interface.

It is recommended, if satisfied with the results after each step, to save the current state with the save as reference button (Fig. 2a). This allows reloading the last satisfactory state of the image process with the reload reference button, in the event that undesired changes are applied in a following step. From the interface, there is the possibility to save the current measurement in comma-separated value (csv) format by creating a new file (save csv) or saving into an already existing file (append in csv file), to facilitate the analysis of data from sets of pictures. When initializing a new csv file, the headings "File Name; px in X mm; Length (mm)" are inserted into the file. Then, there will be a row for each file analysed and appended. A total of three columns are saved. The first will contain the file name of the object of the analysis, the second column is the number of pixels reported for the measured objects, and the third column is the total length in millimetres. If only the "save csv" button is used, a file with two rows (one heading and one result length) and three columns is obtained for the file.

The intervention of the user is required for each picture to be analysed, in order to selectively identify and remove noisy regions (steps 2, 5 and 9) and to separate the object from the background (step 6). These key steps may be reiterated by the user to find the optimal solution (via trial and error—e.g. for thresholding—or with consecutive removal of unwanted areas) in the case of very complex images (e.g. irregular exposure, complex objects).

Validation of *HyLength*

Using the newly developed *HyLength* tool, we determined the lengths of all acquired images and the time needed for each measuring process (from image loading to length recording). The validation of the *HyLength* was performed by comparing the entire root and mycelium measures made with the *HyLength* to manual length measures. For roots and low-density mycelium (in vivo system with *R. irregularis* SW101 and in vitro system with *A. oryzae* ATTC 12891), the manual measures were obtained by direct tracing using the freeware software *ImageJ/Fiji* v.2.0.0 (http://imagej.nih.gov/ij/; Schindelin et al. 2012; Schneider et al. 2012). For high-density mycelium (in vitro system with *R. irregularis*

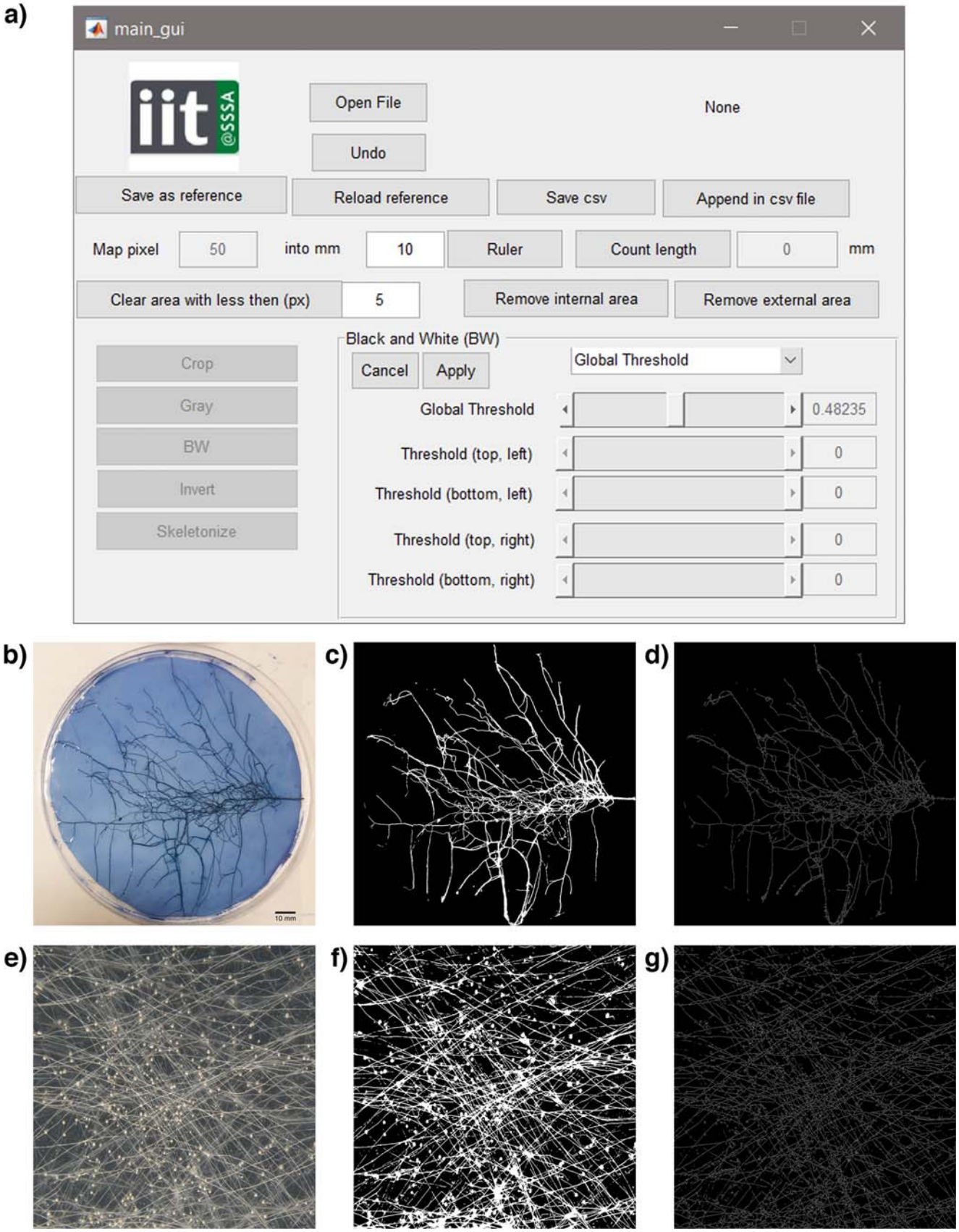
a)
main_gui
Open File
None
Undo
Save as reference
Reload reference
Save csv
Append in csv file
Map pixel
50
into mm
10
Ruler
Count length
0
mm
Clear area with less then (px)
5
Remove internal area
Remove external area
Crop
Gray
BW
Invert
Skeletonize
Black and White (BW)
Cancel
Apply
Global Threshold
Global Threshold
0.48235
Threshold (top, left)
0
Threshold (bottom, left)
0
Threshold (top, right)
0
Threshold (bottom, right)
0
b)
c)
d)
e)
f)
g)

◀ **Fig. 2** User interface of *HyLength* and examples of images processed by the tool. **a** User interface with commands for digital image processing to determine the total length of filamentous structures. **b** Stained root system of *Medicago sativa* L. on nitrocellulose membrane. **c** Roots of **b** following cropping, grey scale and threshold steps. **d** The same roots following skeletonisation. **e** Extraradical mycelium of the arbuscular mycorrhizal (AM) fungus *Rhizophagus irregularis* in a growth medium. **f** The AM fungus mycelium following grey scale and threshold steps. **g** The AM fungus mycelium following skeletonisation

MUCL 41883), the manual measures were obtained by counting intersections with a virtual grid-line, superimposed on the images using the *ImageJ/Fiji* v.2.0.0, and entering the counts into the Newman equation (Newman 1966). We consider high-density mycelia to be those having a hyphal density greater than 2 mm mm^{-2} (Avio et al. 2006; Giovannetti et al. 2006) and greater than 1 m cm^{-3} (St-Arnaud et al. 1996; Warnock et al. 2010). The time needed for measuring lengths by the *HyLength* and by the manual method, from image loading to length recording, was assessed for three independent users with low/medium experience in using the tools. For the *HyLength*, the time required to set the parameters Global Threshold or 4-sub Threshold and clear area with less than (from 1 to 10 px) is included. The parameters of the *HyLength* were optimised for each image with five tests per user.

Benchmarking of *HyLength*

The *AnaMorf* plugin for the *ImageJ/Fiji* is a currently available digital image analysis tool, which allows measuring total fungal hyphal lengths in a fully automated manner starting from a directory of image files or a single file. It allows the user to set default parameters (minimal branch length, maximum circularity, curvature window, noise-reduction filter radius, auto-thresholding method, etc.) for all the images in the directory before image acquisition. We adopted the *AnaMorf* v.2.017 (https://biii.eu/anamorf; Barry et al. 2009, 2015; Barry and Williams 2011) as our benchmarking tool for the *HyLength*. The lengths of all the images measured with the *HyLength* were compared with corresponding *AnaMorf* measurements.

In addition, the lengths determined with the *AnaMorf* were compared with the manual measurements used for validation to get information about the precision and accuracy of this tool. The time needed for measuring the lengths with the *AnaMorf*, from image loading to length recording, was assessed by three independent users with low/medium experience in using the tool. The time required to set the following parameters is included: minimum branch length, maximum circularity, noise-reduction filter radius, selection of threshold method. Default values were maintained for the other parameters. The parameters of the *AnaMorf* were optimised for each set of images with five tests per user.

Statistical analyses

The validation of the *HyLength* was performed comparing the computerised measurements with manual measurements considered the traditional gold standard assay. Regressions of the pair of measurements were performed applying a general linear model (GLM). Moreover, the agreement of values obtained by the *HyLength* versus manual measurements was determined by the concordance correlation coefficient (ρ_c) (Lawrence and Lin 1989) that measures the variation from the 45° line (line of equality) through the origin. Similar analyses were used for the *HyLength* benchmarking against the *AnaMorf* and for *AnaMorf* comparison with the manual measurements. Concordance correlation coefficient values were classified according to Altman (1991). Analysis of variance

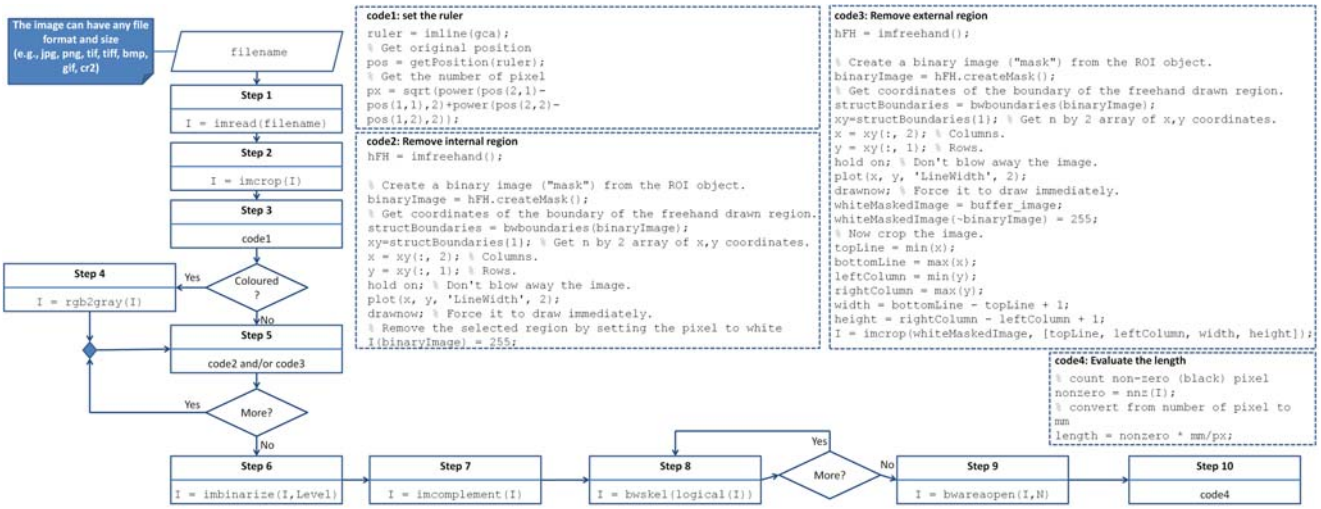

Fig. 3 Flowchart of the developed image analysis tool for measuring root and hypha lengths. The consecutive steps together with concise code lines reporting key functions adopted from the Image Processing Toolbox of MATLAB R2019b (The MathWorks Inc., 2019) are reported

(ANOVA) was performed, after appropriate transformations to fulfil the assumptions of the ANOVA, on the time required for measuring all images with the *HyLength*, manual counting (tracing and grid-line intersection) and *AnaMorf*. The differences between means were determined by the Tukey-*B* test (Rovai et al. 2014). All the analyses were performed with SPSS, v.21.0 (SPSS Inc., Chicago, IL, USA).

Results

Validation of *HyLength* against manual methods

The *HyLength* was validated by comparing measurements of digital images of roots and fungal hyphae with manual methods (Fig. 4). As regards the in vivo two-dimensional system, measurements of *M. sativa* roots and *R. irregularis* hyphal lengths obtained with the *HyLength* were very strongly correlated with the manual tracing measurements ($r = 0.946$, $P < 0.001$, $n = 13$ and $r = 0.987$, $P < 0.001$, $n = 20$, respectively; Fig. 4a, b). The *A. oryzae* hyphal lengths obtained with the *HyLength* in the in vitro system were also very strongly correlated with the measurements obtained by manual tracing ($r = 0.997$, $P < 0.001$, $n = 12$) (Fig. 4c). Along with this, the hyphal lengths of *R. irregularis*, obtained with the *HyLength* in the in vitro system, were very strongly correlated with the measurements obtained by counting the intersections with a virtual grid-line ($r = 0.963$, $P < 0.001$, $n = 25$). All the concordance correlation coefficient (ρ_c) values were higher than 0.81 (from 0.86 to 0.90 for hyphae of *R. irregularis* in the in vivo system and hyphae of *A. oryzae* in the in vitro system, respectively), indicating an almost perfect agreement between the *HyLength* and manual measures for roots as well as for low- and high-density hyphae (Fig. 4). The slopes of the linear regressions reported in Fig. 4 indicated a slight underestimation by the *HyLength* for the roots of *M. sativa* in the in vivo system (12 cm of underestimation per metre) and for the hyphae of *A. oryzae* and *R. irregularis* in the in vitro systems (8.3

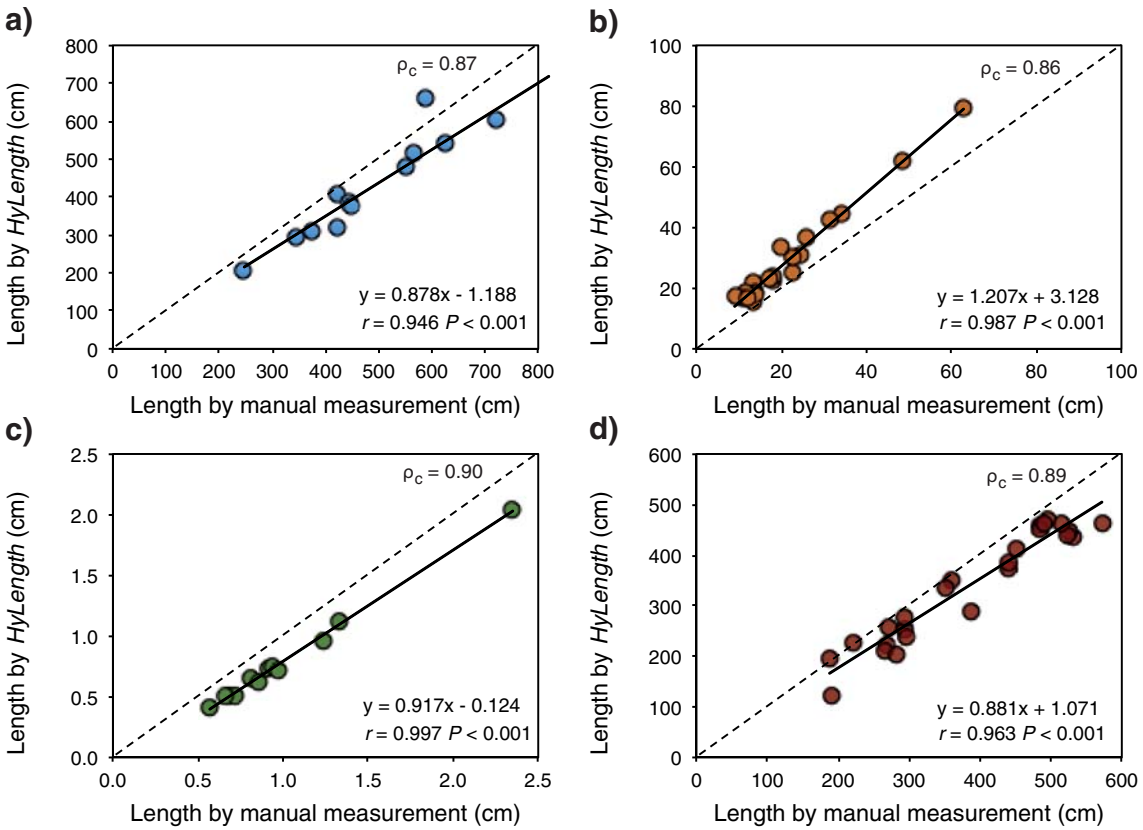

Fig. 4 Linear regressions of root and fungus hyphal lengths measured by *HyLength* and manual methods. **a** *Medicago sativa* roots grown on nitrocellulose membranes ($n = 13$). **b** Low-density, trypan blue–stained mycelia of *Rhizophagus irregularis* growing on nitrocellulose membranes ($n = 20$). **c** Germination hyphae of *Aspergillus oryzae* growing on cellophane ($n = 12$). **d** High-density mycelia of *R. irregularis* growing on transparent modified Strullu and Romand medium ($n = 25$). The manual length measurements for **a**–**c** were done by manually tracing the roots and hyphae in *ImageJ*, while for **d** by manual intersect counting. The equation of the linear regression, *r* correlation coefficients and *P*-values are shown in the right bottom corner of each panel. The concordance correlation coefficient (ρ_c) is shown in the top right corners

and 11.9 cm of underestimation per metre, respectively). Conversely, the *HyLength* overestimated the hyphal measures for hyphae of *R. iregularis* in the in vivo system (20.7 cm of overestimation per metre).

Benchmarking of *HyLength* against *AnaMorf*

Measurements of *M. sativa* roots and *R. irregularis* hyphal lengths, obtained in the in vivo two-dimensional system with the *HyLength*, were medium correlated to *AnaMorf* measurements ($r = 0.872$, $P < 0.001$, $n = 13$ and $r = 0.757$, $P < 0.001$, $n = 20$, respectively; Fig. 5a, b). By contrast, the *A. oryzae* hyphal lengths obtained with the *HyLength* in the in vitro system were very strongly correlated with the measurements obtained with the *AnaMorf* ($r = 0.994$, $P < 0.001$, $n = 12$) (Fig. 5c). Finally, the hyphal lengths of *R. irregularis*, obtained with the *HyLength* in the in vitro system, were medium correlated to the measurements obtained by the *AnaMorf* ($r = 0.829$, $P < 0.001$, $n = 25$) (Fig. 5d). The agreement of the measures taken with the *HyLength* and *AnaMorf* differed according to the experimental system and the measured object. The concordance correlation coefficient (ρ_c) of the *HyLength* measures against the *AnaMorf* measures indicated an almost perfect agreement for the hyphae of *A. oryzae* in the in vitro system, while it showed a moderate and substantial agreement for the in vivo grown *M. sativa* roots and *R. irregularis* hyphae, respectively (Fig. 5). By contrast, the value of ρ_c showed a fair agreement between the *HyLength* against *AnaMorf* measures for the hyphae of *R. irregularis* in the in vitro system (Fig. 5d). The measures of the roots of *M. sativa* in the in vivo system and hyphae of *R. irregularis* in the in vitro system obtained with the *AnaMorf* were less than the *HyLength* measures (Fig. 5a, d).

Additionally, to support our benchmarking, the four sets of measurements (i.e. roots and hyphae in the in vivo system, *A. oryzae* and *R. irregularis* in the two in vitro systems) taken with the *AnaMorf* were validated against manual measurements (Fig. S1). As regards the in vivo two-dimensional system, measurements of *M. sativa* roots and *R. irregularis* hyphal lengths obtained with the *AnaMorf* were medium correlated with the manual tracing measurements ($r = 0.866$, $P < 0.001$, $n = 13$ and $r = 0.787$, $P < 0.001$, $n = 20$,

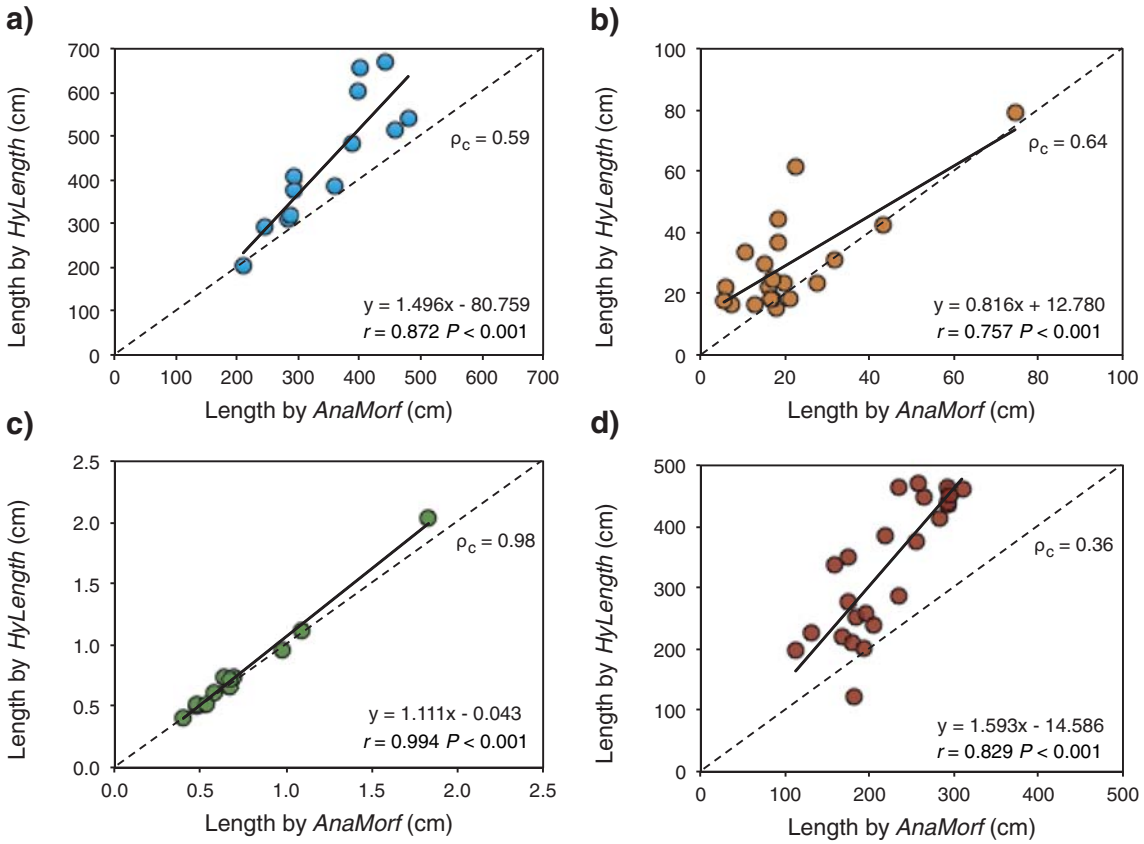

Fig. 5 Linear regressions of root and fungal hyphal lengths measured by *HyLength* and *AnaMorf* tools. **a** *Medicago sativa* roots grown on nitrocellulose membranes ($n = 13$). **b** Low-density, trypan blue–stained mycelia of *Rhizophagus irregularis* growing on nitrocellulose membranes ($n = 20$). **c** Germination hyphae of *Aspergillus oryzae* growing on cellophane ($n = 12$). **d** High-density mycelia of *R. irregularis* growing on transparent modified Strullu and Romand medium ($n = 25$). The equation of the linear regression, r correlation coefficients and P-values are shown in the right bottom corner of each panel. The concordance correlation coefficient (ρ_c) is shown in the top right corners

respectively, Fig. S1a,b). In contrast, the *A. oryzae* hyphal lengths obtained with the *AnaMorf* in the in vitro system were very strongly correlated with the measurements obtained by manual tracing ($r = 0.991$, $P < 0.001$, $n = 12$), whereas *R. irregularis* hyphal lengths obtained with the *AnaMorf* in the in vitro systems were medium correlated with the measurements obtained by manual tracing ($r = 0.909$, $P < 0.001$, $n = 25$) (Fig. S1c, d). The values of ρ_c obtained for the validation of the *AnaMorf* against manual measures indicated a substantial agreement for the hyphae of *R. irregularis* measured in the in vivo system and an almost perfect agreement for the hyphae of *A. oryzae* in the in vitro system (Fig. S1b, c). In contrast, ρ_c indicated a moderate and fair agreement for roots of *M. sativa* in the in vivo system and for hyphae of *R. irregularis* in the in vitro system, respectively (Fig. S1a, d). Accordingly, the slopes of the linear regressions reported in Fig. S1 indicated a strong underestimation by the *AnaMorf* for roots of *M. sativa* in the in vivo system (53.2 cm of underestimation per meter), a slight underestimation for hyphae of *R. irregularis* in the in vivo system (11 cm of underestimation per meter), and a strong underestimation for hyphae of *R. irregularis* grown in the in vitro system (56.7 cm of underestimation per meter) (Fig. S1a, b, d). For the hyphae of *A. oryzae* in the in vitro system, the underestimation was 18.5 cm per m (Fig. S1c).

Time required for length measurements

Compared with manual methods, the *HyLength* tool reduces the time for length measurement of the four sets of images: by 25-fold for *M. sativa* roots in the in vivo system, 34% for *R. irregularis* in the in vivo system, 170% for *A. oryzae* hyphae in the in vitro system and 37% for the *R. irregularis* hyphae in the in vitro system (Fig. 6). The time needed to measure *M. sativa* roots in the in vivo system using the *HyLength* was similar to that using the *AnaMorf* (+ 11%), whereas for *R. irregularis* hyphae in the in vivo system and *A. oryzae* in the in vitro system, the time using the *HyLength* was 3-fold and 35% higher than using the *AnaMorf*, respectively. In contrast, the time needed to measure *R. irregularis* hyphae in the in vitro system using the *HyLength* was reduced by 65% with respect to the *AnaMorf*.

Discussion

Given current interest to infer mechanistic relationships and evolutionary adaptation from phenotypic characteristics of AMF, and that hyphal lengths are still determined manually (Koch et al. 2004; Kokkoris et al. 2019), we identified a need for an image analysis tool able to provide reliable measures and to decrease measuring time. Thus, an image analysis tool named *HyLength* was developed and successfully validated by comparison with manual measurements of four sets of images of roots and hyphae of fungi grown in different experimental systems. The *HyLength* strongly reduced the time needed for image measuring versus manual methods. However, all the validations were performed on experimental set-ups without soil, involving a single AMF species belonging to Glomeromycota (*R. irregularis*) and one species belonging to Ascomycota (*A. oryzae*), in very clean conditions.

HyLength provides object length measures comparable with manual assessment

Validation of the *HyLength* was performed against manual methods using four sets of images, and the accuracy of the measures was high, given correlation coefficients higher than 0.9 and concordance correlation coefficients (ρ_c) greater than 0.8 for all sets of images. For *M. sativa* roots and for *R. irregularis* hyphae in the in vitro system, the *HyLength* underestimated by about 12 cm per m compared with manual methods. The estimation was more precise for *A. oryzae* hyphae (8.3 cm per m of underestimation). The underestimation can occur because of a complex arrangement of the objects, e.g. roots and hyphae with many crossing filaments. Possible causes of underestimation of high-density objects (*M. sativa* roots and hyphae of *R. irregularis* in vitro) are due to the alignment and touching of filaments that are not accurately separated and to object overlap. A strong threshold application might induce loss of details and a consequent underestimation of length, while a weak threshold might lead to artefacts and to overestimation of length. Moreover, underestimation can be even greater in the case of low-contrast images, where objects are not clearly discernible from the background.

The measurements obtained for the hyphae of *R. irregularis* in the in vivo system were overestimated by 20.7 cm per m compared with manual measures. Overestimation can be induced by low resolution of the images, e.g. when not well in focus so the edges of the filaments are not clear and some artefacts can be added to the skeletonised picture. Indeed, overestimation also might be due to non-target objects (i.e. dirt, shadows and reflection). Overall, under- and overestimations can be induced by several factors (e.g. user experience: ability in cleaning artefacts from the images; image contrast and resolution; cloudy not well focused images; complexity of elements: objects crossing each other or presence of spores). Consequently, when diverse and heterogeneous images, varying in object type, resolution and contrast, are to be processed, a flexible tool like the *HyLength*, which allows manual adjustment of operational parameters, is preferred. The utility of

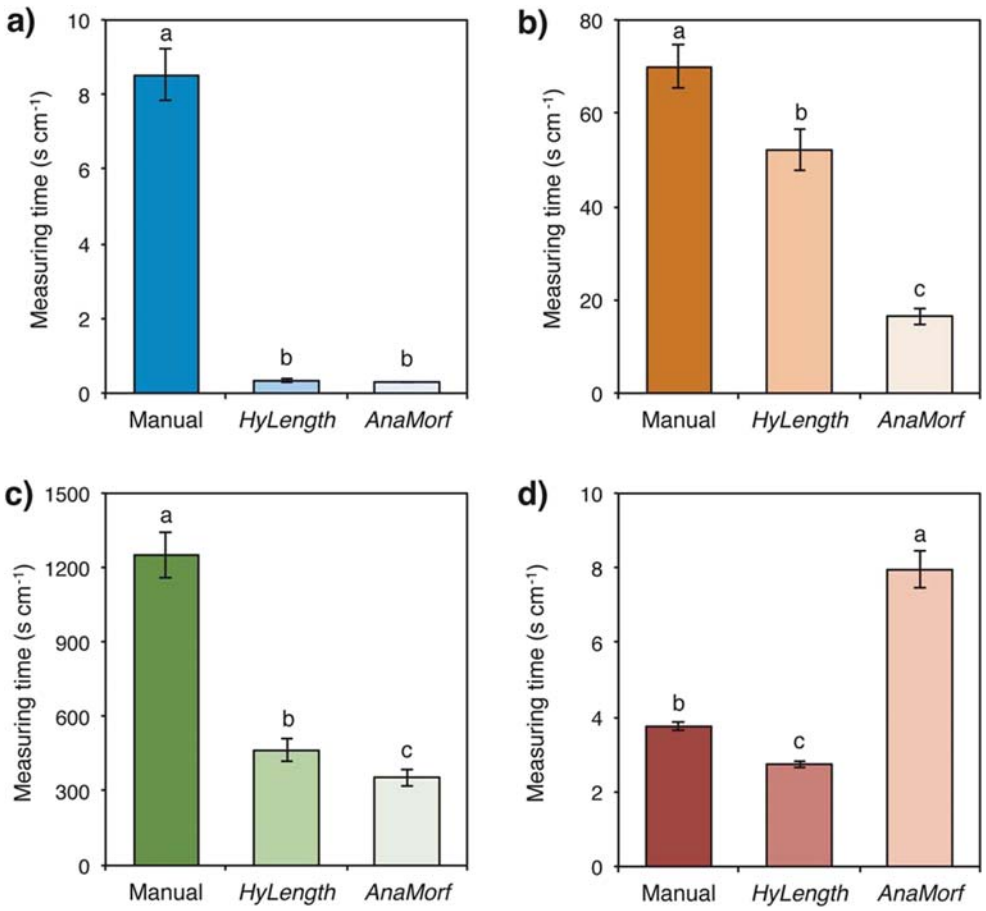

Fig. 6 Mean total processing time (± SE) for the analysis of root and fungal hyphal length of sets of digital images, using manual methods, *HyLength* and *AnaMorf* tools. **a** *Medicago sativa* grown on nitrocellulose membranes ($n = 13$). **b** Low-density, trypan blue–stained mycelia of *Rhizophagus irregularis* growing on nitrocellulose membranes ($n = 20$). **c** Germination hyphae of *Aspergillus oryzae* growing on cellophane ($n = 12$). **d** High-density mycelia of *R. irregularis* growing on transparent modified Strullu and Romand medium ($n = 25$). The manual length measurements in **a**, **b** and **c** were done by manually tracing the roots and hyphae in *ImageJ*, while for **d** by manual intersect counting. Bars topped by the same letter do not differ significantly at $P < 0.05$ by Tukey-B test

semi-automated tools is confirmed by recent published software for root analysis (Lobet et al. 2011; Betegón-Putze et al. 2019). For optimal *HyLength* performance, images should be acquired at moderate-to-high resolution, which is ≥ 72 dpi for roots and ≥ 300 dpi, i.e. 118 px cm^{-1}, for fungal hyphae.

We believe that our tool could be successfully used for hyphae on membrane filters after extraction from soil samples (Jakobsen et al. 1992; Shen et al. 2016). Under such conditions in which dirty images are produced with many non-target objects (debris, soil particles, spores, hyphae of other fungi, etc.), the *HyLength* can be used to selectively identify and remove noisy regions and to separate the target objects from the background. In addition, in heterogeneous images, the *HyLength* allows applying spatially different thresholds for different quadrants and the user can find the optimal solution for each image. The *HyLength* also can be successfully used for AMF species other than *R. irregularis*, such as *Rhizophagus prolifer* which forms profuse branches of very fine hyphae that are hard to assess with the grid-line intersect method. Obviously, high-quality images (high magnification and resolution) should be utilised.

HyLength performs better than *AnaMorf* for complex filamentous objects

Comparing the *HyLength* with *AnaMorf* pointed at a very strong agreement when measurements are taken on the hyphae of *A. oryzae*, as provided by Barry et al. (2009) and originally used to validate the *AnaMorf*. Conversely, the agreement was poor when roots and low- and high-density hyphae of *R. irregularis* were processed. The *HyLength* compared with *AnaMorf* overestimated the roots and the high-density hyphae and underestimated the low-density hyphae. From the comparison of the *AnaMorf* with manual measures of hyphae of *R. irregularis* in the in vitro system, we found that the *AnaMorf* strongly underestimated the length. Thus, we believe that the poor agreement of the *HyLength* with *AnaMorf* is because the *AnaMorf* loses small diameter and poor-contrast structures. In the *AnaMorf*, the complete automatization of the process with multiple image analysis does not allow users to selectively identify and remove noisy regions and to separate the object from the background. Thus, the user cannot find the optimal solution for each image and this causes a strong underestimation. Moreover, in complex images heterogeneous for resolution and contrast, underestimation could even be greater because the *AnaMorf* does not allow applying different thresholds to regions of the image.

HyLength reduces measuring time compared with manual methods

The *HyLength* allows great reduction of the time needed for length measurement compared with manual methods. Time saving in the case of *M. sativa* roots grown in the in vivo system was about 13′ 39″ per m which corresponds to ca. 60′ 31″ for the experimental unit, i.e. a whole membrane (average length 4.43 m). Time saving in the case of *R. irregularis* hyphae in the in vivo system was 29′ 52″ per m. In Avio et al. (2006), the total hyphal length measured in the same in vivo system was 11.7 and 41.1 m for *Funelliformis mosseae* AZ225C and *Rhizophagus intraradices* IMA6, respectively. Assuming those lengths, we could measure the length of the hyphae over the whole membrane saving 5 h 48′ and 20 h 28′, for *F. mosseae* and *R. intraradices*, respectively. Time saving for *A. oryzae* hyphae in the in vitro system was 13′ 8″ per cm which corresponds to 10′ 30″ for a recently germinated spore (average length 0.8 cm; Barry et al. 2015). Time saving for hyphae of *R. irregularis* in the in vitro system was 1′ 41″ per m which corresponds to 60′ 43″ per experimental unit, i.e. Petri plate (average length ca. 36 m; Cardini et al., unpublished data). Therefore, the *HyLength* can allow measurement of the length over a whole experimental unit, eliminating the error due to sub-area selection by the user and allowing processing of many samples.

Compared with the *AnaMorf*, the *HyLength* performed similarly with *M. sativa* roots, whereas it required more time with the hyphae of *R. irregularis* in the in vivo system (59′ 20″ per m) and hyphae of *A. oryzae* in the in vitro system (1′ 48″ per cm). The computational time of the *HyLength* depends on the quality of images; thus, in the presence of a noisy background, the manual cleaning and the adjustment of parameters can be time-demanding. On the other hand, the time needed for the *AnaMorf* plugin is lower than for the *HyLength* because it automatically processes an entire folder of images, while the *HyLength* requires human intervention for each image. Thus, *AnaMorf* speed is a significant advantage when many high-quality images of homogeneous, simple objects are processed. However, we must consider that the use of the *AnaMorf* produced accurate measures for germinating spores of *A. oryzae* and *R. irregularis* in the in vivo system, but produced a strong underestimation of *R. irregularis* in the in vitro system.

The *HyLength* saved time versus the *AnaMorf* in measuring *R. irregularis* hyphae in the in vitro system (8′ 41″ per m, corresponding to 5 h 12′ for a whole Petri plate). Because the processing time in the *AnaMorf* is dependent on the quality of the images and on the complexity of the objects, the speed of the measures is related to computing power (Barry et al. 2015). For these reasons, in the case of the *R. irregularis* hyphae in the in vitro system in which the mycelium is extremely complex, the *AnaMorf* required a long time to produce the skeleton and the length measure. The time needed to set up the *AnaMorf* can be very long because several parameters can be modified before finding the best set of parameters and starting the measuring procedure. Thus, in the *AnaMorf*, the time required per unit length increased proportionally with the increase of the total length, whereas in the HyLength, the time is only slightly increased by the total length and not strictly dependent on the complexity of the object.

Finally, as expected, the *AnaMorf* was faster than manual methods for all sets of images, except for images of the hyphae of *R. irregularis* in the in vitro system. Indeed, for fungal hyphae of dense mycelia, such as the complex network of *R. irregularis*, the *AnaMorf* length measures are strongly underestimated, while the *HyLength* proved to be a fast and accurate tool in accordance with the benchmarking of the *HyLength* versus *AnaMorf*.

In synthesis, the main pros of the *HyLength* can be summarised as follows: (1) the involvement of the users in the semi-automated, instead of fully automated image processing, reduces and prevents possible analytical artefacts; (2) the users do not need lengthy training to use the tool, and a standard office laptop is sufficient to measure even many images; (3) the tool was tested with complex images of fungal hyphae of a mycorrhizal fungus and roots, but because parameters can be optimised by the user, the tool also allows users to work with different, heterogeneous and modest-quality images; (4) the tool reduces the measuring time compared with the manual methodologies, maintaining good accuracy in the estimation of hyphal length; (5) the tool is freely released together with the source code and expert users can implement additional functions and improve the code if necessary. Indeed, users not holding MATLAB licenses can freely download MATLAB Runtime (HyLength requires MATLAB Runtime R2019b https://it.mathworks.com/products/compiler/matlab-runtime.html) to use the *HyLength*.

Conclusions

We have introduced a purpose-built and hence easy to use image tool to measure the length of roots and fungal hyphae. Given there is enough object-to-background contrast, minimal shadow and sufficient image resolution, the lengths are accurate and reproducible. User intervention at each step of image processing ensures that reliable data can be obtained from diverse and even heterogeneous image material. Moreover, the *HyLength* is easy to use by any new or infrequent user. The application of the *HyLength* on the images captured from the in vitro system with Z-stack imaging allowed the determination of the whole length of three-dimensional complex mycelia. This supports the use of the *HyLength* for plant-fungus phenotyping, relieving scientists from tedious repetitive work and cutting the time for data acquisition.

Author contributions AC, EP and LE planned and designed the research; AC performed the research; EDD designed the software tool; AC collected the data; AC, EP and LE analysed and interpreted the data; and AC, EP, EDD, HG, BM and LE wrote the manuscript.

Funding information We acknowledge the Italian Institute of Technology (IIT) for funding the PhD Fellowship of AC under the PhD programme in Agrobiosciences at the Scuola Superiore Sant'Anna of Pisa, Italy.

References

Allen MF, Kitajima K (2013) *In situ* high-frequency observations of mycorrhizas. New Phytol 200:222–228. https://doi.org/10.1111/nph.12363

Allen JW, Shachar-Hill Y (2009) Sulfur transfer through an arbuscular mycorrhiza. Plant Physiol 149:549–560. https://doi.org/10.1104/pp.108.129866

Altman DG (1991) Practical statistics for medical research. Chapman and Hall, London and New York

Arsenault JL, Poulcur S, Messier C, Guay R (1995) WinRHlZO™, a root-measuring system with a unique overlap correction method. HortScience 30:906. https://doi.org/10.21273/HORTSCI.30.4.906D

Augé RM (2004) Arbuscular mycorrhizae and soil/plant water relations. Can J Soil Sci 84:373–381. https://doi.org/10.4141/S04-002

Avio L, Pellegrino E, Bonari E, Giovannetti M (2006) Functional diversity of arbuscular mycorrhizal fungal isolates in relation to extraradical mycelial networks. New Phytol 172:347–357. https://doi.org/10.1111/j.1469-8137.2006.01839.x

Bago B, Pfeffer PE, Shachar-Hill Y (2000) Carbon metabolism and transport in arbuscular mycorrhizas. Plant Physiol 124:949–958. https://doi.org/10.1104/pp.124.3.949

Barry DJ, Williams GA (2011) Microscopic characterisation of filamentous microbes: towards fully automated morphological quantification through image analysis. J Microsc-Oxford 244:1–20. https://doi.org/10.1111/j.1365-2818.2011.03506.x

Barry DJ, Chan C, Williams GA (2009) Morphological quantification of filamentous fungal development using membrane immobilization and automatic image analysis. J Ind Microbiol Biot 36:787–800. https://doi.org/10.1007/s10295-009-0552-9

Barry DJ, Williams GA, Chan C (2015) Automated analysis of filamentous microbial morphology with AnaMorf. Biotechnol Prog 31:849–852. https://doi.org/10.1002/btpr.2087

Betegón-Putze I, González A, Sevillano X, Blasco-Escámez D, Caño-Delgado AI (2019) My ROOT: a method and software for the semi-automatic measurement of primary root length in Arabidopsis seedlings. Plant J 98:1145–1156. https://doi.org/10.1111/tpj.14297

Brunk M, Sputh S, Doose S, van de Linde S, Terpitz U (2018) HyphaTracker: an ImageJ toolbox for time-resolved analysis of spore germination in filamentous fungi. Sci Rep 8:605. https://doi.org/10.1038/s41598-017-19103-1

Bürkert B, Robson A (1994) ^{65}Zn uptake in subterranean clover (*Trifolium subterraneum* L.) by three vesicular-arbuscular mycorrhizal fungi in a root-free sandy soil. Soil Biol Biochem 26:1117–1124. https://doi.org/10.1016/0038-0717(94)90133-3

Coccina A, Cavagnaro TR, Pellegrino E, Ercoli L, McLaughlin MJ, Watts-Williams SJ (2019) The mycorrhizal pathway of zinc uptake contributes to zinc accumulation in barley and wheat grain. BMC Plant Biol 19:133. https://doi.org/10.1186/s12870-019-1741-y

Cranenbrouck S, Voets L, Bivort C, Renard L, Strullu DG, Declerck S (2005) Methodologies for in vitro cultivation of arbuscular mycorrhizal fungi with root organs. In: Declerck S, Fortin JA, Strullu D (eds) In vitro culture of mycorrhizas. Springer, Berlin, pp 341–375. https://doi.org/10.1007/3-540-27331-X_18

Declerck S, Strullu DG, Plenchette C (1998) Monoxenic culture of the intraradical forms of Glomus sp. isolated from a tropical ecosystem: a proposed methodology for germplasm collection. Mycologia 90:579–585. https://doi.org/10.1080/00275514.1998.12026946

Dhondt S, Van Haerenborgh D, Van Cauwenbergh C, Merks RM, Philips W, Beemster GT, Inzé D (2012) Quantitative analysis of venation patterns of Arabidopsis leaves by supervised image analysis. Plant J 69:553–563. https://doi.org/10.1111/j.1365-313X.2011.04803.x

Ercoli L, Schüßler A, Arduini I, Pellegrino E (2017) Strong increase of durum wheat iron and zinc content by field-inoculation with arbuscular mycorrhizal fungi at different soil nitrogen availabilities. Plant Soil 419:153–167. https://doi.org/10.1007/s11104-017-3319-5

George E, Marschner H, Jakobsen I (1995) Role of arbuscular mycorrhizal fungi in uptake of phosphorus and nitrogen from soil. Crit Rev Biotechnol 15:257–270. https://doi.org/10.3109/07388559509147412

Giovannetti M, Avio L, Fortuna P, Pellegrino E, Sbrana C, Strani P (2006) At the root of the wood wide web: self recognition and nonself incompatibility in mycorrhizal networks. Plant Signal Behav 1:1–5. https://doi.org/10.4161/psb.1.1.2277

Green DC, Newsam R, Jeffries P, Dodd JC, Vilariño A (1994) Quantification of mycelial development of arbuscular mycorrhizal fungi using image analysis. Mycorrhiza 5:105–113. https://doi.org/10.1007/BF00202341

Himmelbauer ML (2004) Estimating length, average diameter and surface area of roots using two different image analyses systems. Plant Soil 260:111–120. https://doi.org/10.1023/B:PLSO.0000030171.28821.55

Hodge A, Helgason T, Fitter AH (2010) Nutritional ecology of arbuscular mycorrhizal fungi. Fungal Ecol 3:267–273. https://doi.org/10.1016/j.funeco.2010.02.002

Jakobsen I, Abbott LK, Robson AD (1992) External hyphae of vesicular-arbuscular mycorrhizal fungi associated with *Trifolium subterraneum* L. 1. Spread of hyphae and phosphorus inflow into roots. New Phytol 120:371–380. https://doi.org/10.1111/j.1469-8137.1992.tb01077.x

Koch AM, Kuhn G, Fontanillas P, Fumagalli L, Goudet J, Sanders IR (2004) High genetic variability and low local diversity in a population of arbuscular mycorrhizal fungi. P Natl Acad Sci USA 101:2369–2374. https://doi.org/10.1073/pnas.0306441101

Koide RT, Mosse B (2004) A history of research on arbuscular mycorrhiza. Mycorrhiza 14:145–163. https://doi.org/10.1007/s00572-004-0307-4

Kokkoris V, Miles T, Hart MM (2019) The role of in vitro cultivation on asymbiotic trait variation in a single species of arbuscular mycorrhizal fungus. Fungal Biol-UK 123:307–317. https://doi.org/10.1016/j.funbio.2019.01.005

Lawrence I, Lin K (1989) A concordance correlation coefficient to evaluate reproducibility. Biometrics:255–268. https://doi.org/10.2307/2532051

Lehmann A, Rillig MC (2015) Arbuscular mycorrhizal contribution to copper, manganese and iron nutrient concentrations in crops–a meta-analysis. Soil Biol Biochem 81:147–158. https://doi.org/10.1016/j.soilbio.2014.11.013

Li XL, Marschner H, George E (1991) Acquisition of phosphorus and copper by VA-mycorrhizal hyphae and root-to-shoot transport in white clover. Plant Soil 136:49–57. https://doi.org/10.1007/BF02465219

Liu A, Hamel C, Hamilton RI, Ma BL, Smith DL (2000) Acquisition of Cu, Zn, Mn and Fe by mycorrhizal maize (*Zea mays* L.) grown in soil at different P and micronutrient levels. Mycorrhiza 9:331–336. https://doi.org/10.1007/s005720050277

Lobet G (2017) Image analysis in plant sciences: publish then perish. Trends Plant Sci 22:559–566. https://doi.org/10.1007/BF02465219

Lobet G, Pagès L, Draye X (2011) A novel image-analysis toolbox enabling quantitative analysis of root system architecture. Plant Physiol 157:29–39. https://doi.org/10.1104/pp.111.179895

Lobet G, Draye X, Périlleux C (2013) An online database for plant image analysis software tools. Plant Methods 9:38. https://doi.org/10.1186/1746-4811-9-38

Mathworks Inc (2019) MATLAB version 9.7.0.1165820 (R2019b). Natick, Massachusetts

Meijering E, Jacob M, Sarria JC, Steiner P, Hirling H, Unser M (2004) Design and validation of a tool for neurite tracing and analysis in fluorescence microscopy images. Cytom Part A 58:167–176. https://doi.org/10.1002/cyto.a.20022

Miransari M, Bahrami HA, Rejali F, Malakouti MJ (2009) Effects of soil compaction and arbuscular mycorrhiza on corn (*Zea mays* L.) nutrient uptake. Soil Till Res 103:282–290. https://doi.org/10.1016/j.still.2008.10.015

Naeem A, French AP, Wells DM, Pridmore TP (2011) High-throughput feature counting and measurement of roots. Bioinformatics 27:1337–1338. https://doi.org/10.1093/bioinformatics/btr126

Newman EI (1966) A method of estimating the total length of root in a sample. J Appl Ecol:139–145. https://doi.org/10.2307/2401670

Pellegrino E, Ramasamy CK, Sbrana C, Barberi P, Giovannetti M (2010) Selection of infective arbuscular mycorrhizal fungal isolates for field inoculation. Ital J Agron:225–232. https://doi.org/10.4081/ija.2010.225

Pierret A, Gonkhamdee S, Jourdan C, Maeght JL (2013) IJ_Rhizo: an open-source software to measure scanned images of root samples. Plant Soil 373:531–539. https://doi.org/10.1007/s11104-013-1795-9

Qi X, Qi J, Wu Y (2007) RootLM: a simple color image analysis program for length measurement of primary roots in Arabidopsis. Plant Root 1:10–16. https://doi.org/10.3117/plantroot.1.10

Rose L, Lobet G (2019) Accuracy of image analysis tools for functional root traits: a comment on Delory et al. (2017). Methods Ecol Evol 10:702–711. https://doi.org/10.1111/2041-210X.13156

Rovai AP, Baker JD, Ponton MK (2014) Social science research design and statistics: a practitioner's guide to research methods and IBM SPSS. Watertree Press LLC, Chesapeake

Schindelin J, Arganda-Carreras I, Frise E, Kaynig V, Longair M, Pietzsch T, Preibisch S, Rueden C, Saalfeld S, Schmid B, Tinevez JY, White DJ, Hartenstein V, Eliceiri K, Tomancak P, Cardona A (2012) Fiji: an open-source platform for biological-image analysis. Nat Methods 9:676–682. https://doi.org/10.1038/nmeth.2019

Schneider CA, Rasband WS, Eliceiri KW (2012) NIH image to ImageJ: 25 years of image analysis. Nat Methods 9:671–675. https://doi.org/10.1038/nmeth.2089

Schüßler A, Walker C (2010) The Glomeromycota: a species list with new families and new genera. The Royal Botanic Garden Edinburgh, The Royal Botanic Garden Kew, Botanische Staatssammlung Munich, and Oregon State University

Shen Q, Kirschbaum MU, Hedley MJ, Arbestain MC (2016) Testing an alternative method for estimating the length of fungal hyphae using photomicrography and image processing. PLoS One 11:e0157017. https://doi.org/10.1371/journal.pone.0157017

Smith SE, Read DJ (2008) Mycorrhizal symbiosis. Academic Press, Cambridge

Smith SE, Smith FA (2012) Fresh perspectives on the roles of arbuscular mycorrhizal fungi in plant nutrition and growth. Mycologia 104:1–13. https://doi.org/10.3852/11-229

Smith SE, Gianinazzi-Pearson V, Koide R, Cairney JWG (1994) Nutrient transport in mycorrhizas: structure, physiology and consequences for efficiency of the symbiosis. Plant Soil 159:103–113. https://doi.org/10.1007/BF00000099

St-Arnaud M, Hamel C, Vimard B, Caron M, Fortin JA (1996) Enhanced hyphal growth and spore production of the arbuscular mycorrhizal fungus *Glomus intraradices* in an in vitro system in the absence of host roots. Mycol Res 100:328–332. https://doi.org/10.1016/S0953-7562(96)80164-X

Tibbett M (2000) Roots, foraging and the exploitation of soil nutrient patches: the role of mycorrhizal symbiosis. Funct Ecol 14:397–399. https://doi.org/10.1046/j.1365-2435.2000.00417.x

van Vuuren MM, Robinson D, Fitter AH, Chasalow SD, Williamson L, Raven JA (1997) Effects of elevated atmospheric CO2 and soil water availability on root biomass, root length, and N, P and K uptake by wheat. New Phytol 135:455–465. https://doi.org/10.1046/j.1469-8137.1997.00682.x

Voets L, Dupré de Boulois H, Renard L, Strullu DG, Declerck S (2005) Development of an autotrophic culture system for the in vitro mycorrhization of potato plantlets. FEMS Microbiol Lett 248:111–118. https://doi.org/10.1016/j.femsle.2005.05.025

Warnock DD, Mummey DL, McBride B, Major J, Lehmann J, Rillig MC (2010) Influences of non-herbaceous biochar on arbuscular mycorrhizal fungal abundances in roots and soils: results from growth-chamber and field experiments. Appl Soil Ecol 46:450–456. https://doi.org/10.1016/j.apsoil.2010.09.002

Zhang H, Wei S, Hu W, Xiao L, Tang M (2017) Arbuscular mycorrhizal fungus *Rhizophagus irregularis* increased potassium content and expression of genes encoding potassium channels in *Lycium barbarum*. Front Plant Sci 8:440. https://doi.org/10.3389/fpls.2017.00440